STRENGTH ANALYSIS OF SUBSOILER TOOTH

Jacek Caban, Aleksander Nieoczym, Leszek Krzywonos
Lublin University of Technology, Poland
j.caban@pollub.pl, a.nieoczym@pollub.pl, l.krzywonos@pollub.pl

Abstract. Working with a subsoiler is an agro-amelioration procedure consisting in loosening the soil without turning it over, at a depth greater than the depth of plowing with a traditional plow. Subsoiling is intended to loosen excessively compacted layers of the soil profile in order to rebuild its porous structure ensuring proper circulation of water and air in the soil. The operation of agricultural machines for field tasks, including soil loosening and plowing, involves wear and tear of the main working elements. The wear mechanism depends on the loads, the working environment, including the type of soil and possible contamination, e.g. in the form of stones. The article presents solid models and strength analyses using the finite element method. The aim was to compare the influence of the tooth shape: an arched tooth shape and an intermediate tooth shape combining the features of an arched tooth with a flat tooth. Simulations of the working environment concerned loads when loosening light and heavy soil and when hitting a non-deformable element. The issue of the influence of the tooth shape on its strength was solved during the simulation of the operation of the subsoiler. In an arched tooth and a tooth with the characteristics of an arched and straight tooth, stresses of similar values are generated. Differences appear on surfaces with geometric notch features. The greatest differences were noted when simulating a tooth hitting a stone, in which case the arch tooth would be damaged.

Keywords: finite element method, subsoiler, tooth shape, stress map, simulation.

Introduction

As it is known, one of the main indicators of the reliability of various machine parts is wear resistance [1-3]. The literature includes works on the reliability and wear of agricultural machines [4-7], the efficiency and effectiveness of agricultural tractors [8; 9] and their equipment [10; 11] and vehicle components [12-15]. In order to properly select a wear-resistant material, various information should be taken into account, including the working environment, as well as the type of abrasive materials [3; 16; 17]. The use of various types of analyses such as CAD and the Finite Element Method (FEM) is helpful in this selection. Engineers use the support of FEM for analyses when designing machine elements [18-20], motor vehicles [21-23], specialized means of transport [24-26] and agricultural machines [27-29], as well as technological processes [30-32].

Working with a subsoiler is an agro-amelioration procedure consisting in loosening the soil without turning it over, at a depth greater than the depth of plowing with a plow. Subsoiling is intended to loosen excessively compacted layers of the soil profile in order to rebuild the porous structure ensuring proper water and air circulation in the soil. The external symptoms of excessively compacted soil include ponding of water that persists in the field for a long time after heavy rainfall [33; 34]. The main disadvantage of subsoiling is its high energy consumption. The power requirement, with a working depth in the range of 450-600 mm, is 25-35 kW per 1 tooth of the subsoiler, and fuel consumption is estimated at approximately 20-30 liters of diesel oil per 1 hectare [35]. However, this outlay can be compensated by eliminating plowing and increasing yields, especially in dry years or with too intense rainfall.

Scientific research on the use of subsoiler concerns two issues. The first is the efficiency of soil loosening, the second is the optimization of the tooth structure in order to increase its strength and reduce the energy consumption of subsoiling.

Conventional experimental methods regarding the displacement of soil layers are time-consuming and do not allow for a full description of the process of loosening deep soil layers. Therefore, numerical simulation methods are used to digitally model this process. FEM is mainly used for problems of interaction between the subsoiler tooth and the soil with continuous and homogeneous parameters [35]. DEM (Discrete Element Method) can simulate microscale deformations of discontinuous media such as soil particles [36; 37]. The use of both of these numerical methods requires assigning mechanical properties to the soil model [38]. This type of research issues was presented in publications [39-42] where the analysis of stresses in heterogeneous soil was related to the estimation of the power requirement of the engine intended for subsoiling and reducing its pulling force. An additional effect was the optimization of the shape and dimensions of the subsoiler tooth.

Due to the fact that the effectiveness of the subsoiling procedure is influenced by the spatial diversity of the soil, the shape of the tool and the dynamics of tillage machines, a mathematical and analytical model of this process is presented in [43]. The use of input data describing the mechanical properties of the soil and the parameters of the agricultural tractor makes it possible to obtain mathematical equations describing the shape of the tooth of the arch subsoiler. The results of the research aimed at optimizing the shape of subsoiler teeth are included in publications [44; 45]. Teeth from existing subsoil pits are subjected to testing. The result of these studies is an analysis of stress distribution and a description of the verification of experimental results during field tests. Design solutions for deeper teeth other than the conventionally used arched and straight teeth are being sought. The article [46] presents the results of strength tests of a modified tooth with a radial shaft shape, characterized by increased thickness and the lack of a separate structural chisel. The authors of publications [44; 47] included results related to model and field tests of a complete subsoiler. It was assumed that the tine spacing and the number of rows with tines are the parameters determining the soil loosening process expressed by the subsoiling efficiency index (which is a critical performance indicator of subsoiling). The thesis was put forward and proven that the tooth spacing is a key parameter when designing subsoilers and has a significant impact on the range of displacements in the soil layers.

This work presents solid models, strength analyses were performed using FEM. The main purpose of the analysis is to compare the influence of tooth shape: an arched profile and an intermediate one combining the features of an arched tooth with a flat one. Simulations of the working environment concerned loads when loosening light and heavy soil and when hitting a non-deformable element.

Materials and methods

The tests were carried out on the teeth of subsoilers from two manufacturers marked as A and B (Fig. 1). Both devices are equipped with three teeth of the same length. Therefore, they work at the same depth and require similar power requirements. The differentiating feature is the shape of the tooth. In the case of company A, the machine has arc tines in which the width of the shaft increases from the coulter to the mounting points on the frame. Company B uses a tooth profile that is intermediate between a straight and an arched tooth. In this case, the shaft is smaller than in the design of company A, but it is inclined in relation to the base.

a) b)

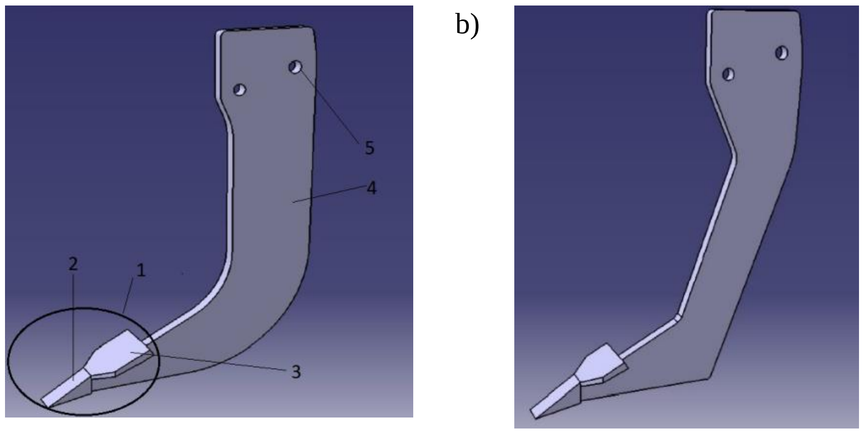

Fig. 1. **Solid models of subsoiler teeth:** a – producer A; b – producer B; 1 – coulter; 2 – chisel; 3 – side undercutters (wings); 4 – shank; 5 – holes for the screws securing the tine to the frame

The coulter mounted on the shaft of the arch tooth is more forward compared to the design of straight teeth. Increasing the protrusion causes the soil to be loosened more intensively and rise to the surface in front of the tooth shaft, reducing the resistance to its movement in the soil. An unfavorable design feature of the arch teeth is the phenomenon of moving hard fragments of soil cut by the coulter and stones along the leading edge of the shaft upwards towards the surface. The zone of soil loosened by a single tine with a straight or arched shaft depends on the width of the coulter. Standardly, coulters with narrow chisels and side undercutters (wings) are used.

The aim of the study was to indicate the relationship between the tooth structure and its strength.

The solid models were made in the Catia V5 program, while the strength analysis using the finite element method (FEM) was carried out in the Abaqus program. Numerical tests simulated real conditions occurring during field work:

- soil loosening,
- hitting a stone with the frontal plane of the tooth chisel.

The subsoiler teeth of both manufacturers are made of S355JR structural steel with a yield strength of *Re* = 355 MPa. For the purposes of strength analysis, it was assumed that solid models are deformable bodies made of isotropic material that deforms in the elastic-plastic range. A hex mesh with C3D8R solid elements was applied to both models. Global mesh density of 10, a mesh of 3 was used on the surfaces reflecting the thickness. The number of finite elements and nodes in the tooth of company A was 2360 and 3853, respectively, in the tooth of company B 1886 and 3118.

Simulation of soil loosening

The load in the form of soil resistance forces was replaced by a force evenly distributed over the chisel surface. Its value of 12,000 N was adopted based on literature data [30; 36; 40]. The load was applied iteratively until it reached its maximum value while moving the tooth over a distance of 100 mm. Assuming that the analysis may be geometrically non-linear, the minimum increment was set at 0.00001% of the entire load.

The distributions of reduced stresses for both analysed subsoiler teeth are shown in Fig. 2. The maximum values occur in the upper part of the tooth body in the plane of change in the cross-sectional area and are 81.27 MPa for the tooth from company B and 53.19 MPa for the structure from company A, respectively. Percentage of the difference in stress values reaches 35%. It results from the geometry of shaping this plane and the formation of a geometric notch. Smaller values are generated in the case of an arcuate transition with a large rounding radius. The maximum stresses do not exceed the yield strength of the material having a value of *Re* = 355 MPa. Stresses of approximately 24 MPa are generated on the front surface of the arch tooth chisel and are twice as high as the stresses on the B tooth chisel.

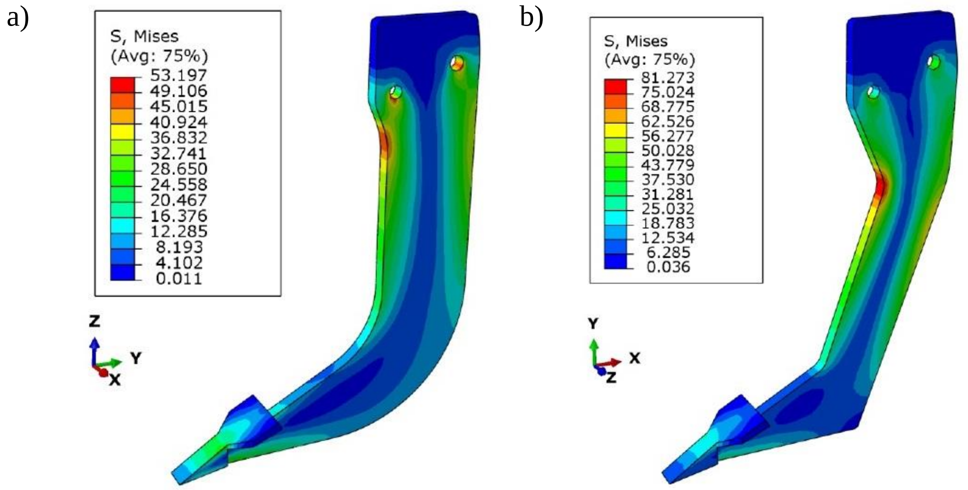

Fig. 2. **Stress maps for the case of loading with a force distributed on the chisel surface:** a – producer A; b – producer B

Another simulation of soil loosening was performed after placing the solid tooth model in the space to which soil properties were assigned. It was assumed that it is a deformable body and belongs to solid elements. The properties of soil as an isotropic material with elastic-plastic deformation features are summarized in Table 1.

To facilitate the discretization of the assembly, partitioning was performed – Fig. 3. A simplification was used that at the moment of initial cooperation, the tooth was already inside an isolated space constituting the soil [29; 36]. C3D8R solid elements with a hex mesh with a density of 38 were used for discretization. The object after discretization had 22,820 finite elements and 25,106 nodes.

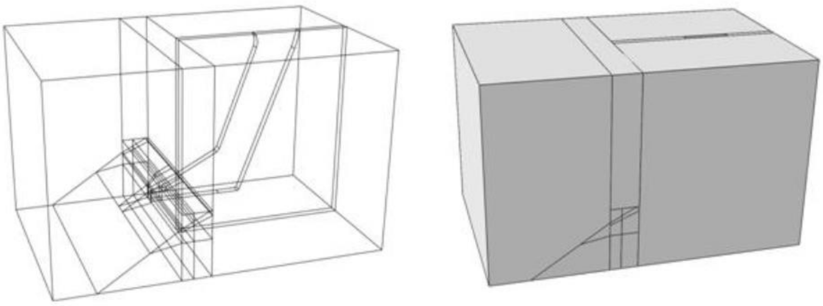

Fig. 3. **Partitioning on a tooth and soil model assembly**

Table 1

Soil strength parameters based on [42; 45]

No.	**Yield stress, MPa**	**Plastic strain, MPa**
1	0.076	0
2	0.77	0.0036
Young's modulus, MPa		**Poisson'ratio**
10		0.35

Surface-to-surface contact between the tooth and the soil, with a slave-master option. The contact property is hard contact with no friction. The strength analysis was solved with an iterative increase in the value of the loading force while moving the tooth over a length of 50 mm [29; 34]. After performing the simulation, reduced stress maps were generated – Fig. 4. The results indicate that both simulations of the soil loosening process led to maximum stress values in the same areas of the tooth shaft. The difference between the values in both types of analyses is approximately 5%.

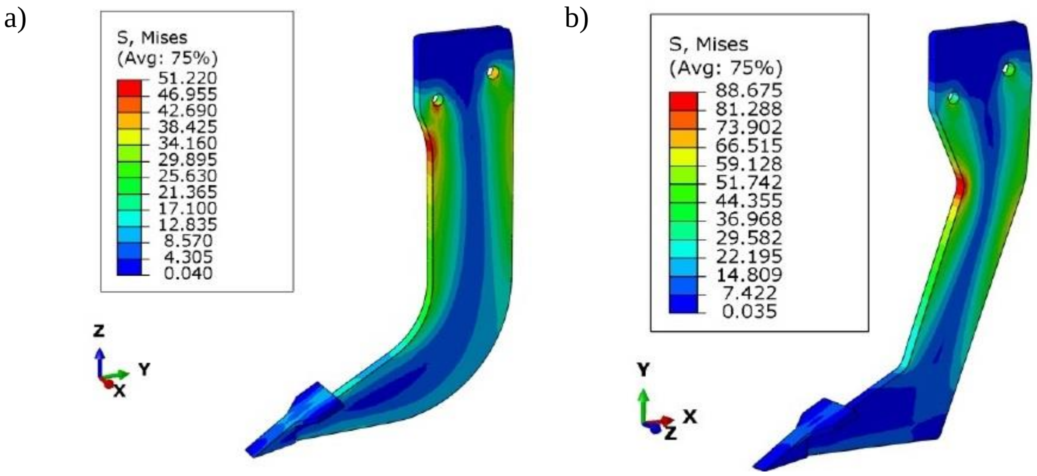

Fig. 4. **Stress maps for loading with a medium-gravity soil model:**
a – producer A; b – producer B

The strength analysis carried out (Fig. 4) reflected the effects of the load acting on the subsoiler teeth when working on medium-heavy soils. In order to additionally check the strength parameters of the teeth, an analysis was carried out using a model reflecting the parameters of heavy soil – Fig. 5. Heavy clay soils are characterized by the Young's modulus of E = 80 MPa, which is the highest value among cohesive soils.

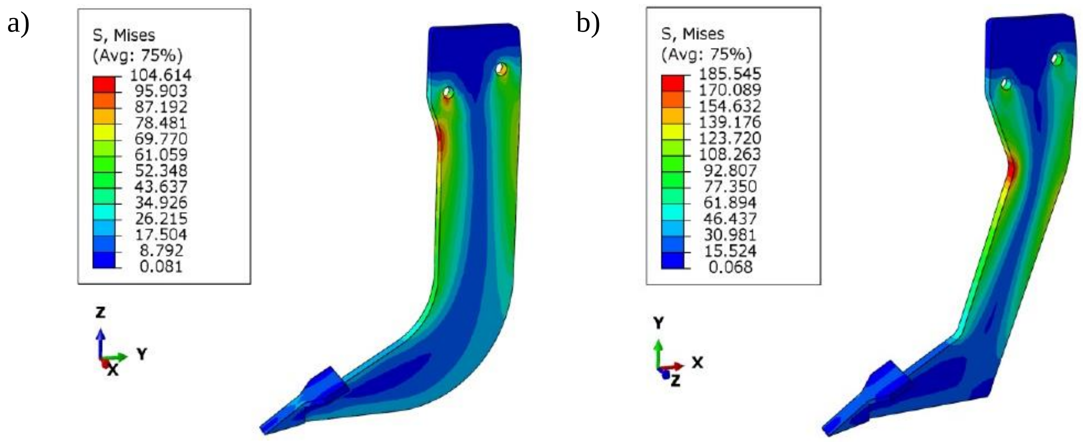

Fig. 5. **Stress maps in the case of heavy soil model loading:** a – producer A; b – producer B

The stress distribution on the tooth surfaces is similar to the maps shown in Fig. 2 and Fig. 4. The areas of maximum values do not change their position, but the values on the surfaces of both structures increased. The reduced stresses on the tooth of the subsoiler from company A changed from 51 to 104 MPa. On the tooth of company B, the maximum stresses reached 185 MPa, which corresponds to half the yield strength of the material.

The results of the performed numerical analyses allow the conclusion that the teeth are made in such a way that the permissible stresses are not exceeded, and therefore they will not be destroyed under loads much higher than those expected during standard field work.

Simulation of collision with an obstacle located in the soil

The case of the impact of a subsoiler tooth on a stone located in the soil, which does not change its position, was analyzed. The stone was modeled as a non-deformable discrete rigid body with the parameters of solid elements. No material characteristics have been assigned to the stone due to the fact that it is a non-deformable element. Surface-to-surface contact was assigned between the interacting elements with the hard contact attribute in the absence of friction.

The stone model was described with elements marked R3D4 with a global mesh density of 38. After discretization, the assemblies had 10,285 finite elements and 7,304 nodes. At the beginning of the strength analysis, the tooth was located at a distance of 25 mm from the stone. It was observed that stresses exceeding the yield strength for S355J steel (Re = 355 MPa) are generated in the front areas of the chisels from both manufacturers, causing permanent deformation of the chisel. Areas with stress values close to the yield point are also observed in the upper part of the shaft near the area of increasing its width.

Analysing the stress maps on the tooth surfaces shown in Figs. 2, 4 and 5, it can be concluded that the design of company A is characterized by greater stiffness. In each of the simulation cases, lower values of reduced stresses were generated on the shank and the share compared to the design of company B. This fact is the result of the fact that when hitting a non-deformable obstacle, the front part of the chisel was deformed (Fig. 6). Additionally, the upper surface of the coulter is the area where the maximum stress values were observed – 510 MPa.

In the tooth from company B, the greatest changes in stress maps occur in the lower, triangular part of the shaft, with stresses of approximately 300 MPa. The stress distribution along the entire length of the tooth shaft of company A has a shape similar to that in a bending beam. In structure B, the locations of the stress maps correspond to the accumulations occurring at the points of the geometric notch. The analysed case presents an extreme situation in which the teeth are attached to the subsoiler frame with screws. In fact, the teeth are fastened using overload protection elements in the form of breakaway screws.

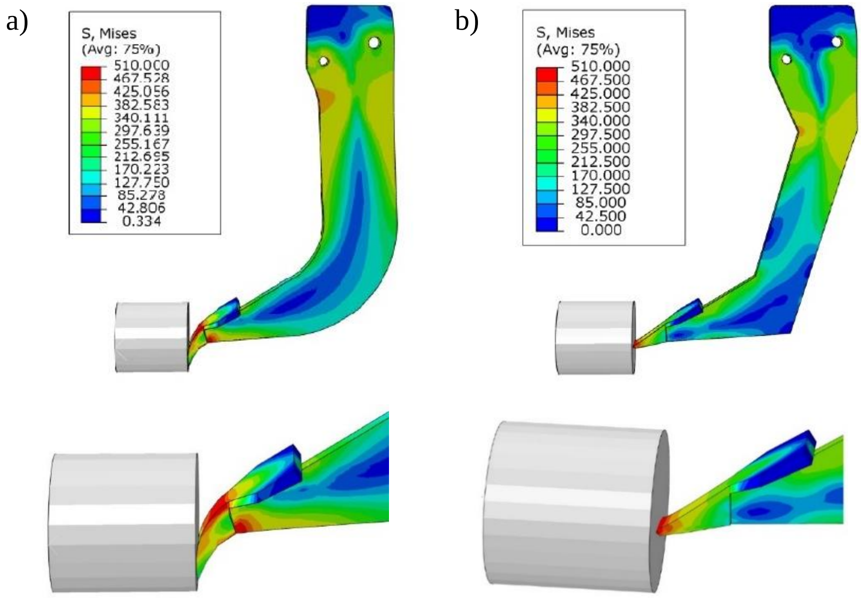

Fig. 6. **Stress maps in the event of a tooth hitting a non-deformable obstacle:**
a – producer A; b – producer B

Conclusions

The performed numerical analyses allow for the formulation of conclusions regarding two research areas: the methodology of the work carried out and the strength of the subsoiler teeth.

1. Simulation of the soil loosening process using a soil model and an equivalent load applied directly to the surface of the coulter and shaft allows for obtaining consistent results. The difference in stress values is approximately 5%. The use of a soil model requires strength parameters closely related to the type of the soil and its physical condition. This type of data is rarely provided in the scientific literature and is often related to specific soils subject to cultivation, e.g. sugar cane.
2. The issue of the influence of the tooth shape on its strength was solved during the simulation of the operation of the subsoiler. In an arched tooth and a tooth with the characteristics of an arched and straight tooth, stresses of similar values are generated. Differences appear on surfaces with geometric notch features. The greatest differences were noted when simulating a tooth hitting a stone, in which case the arch tooth would be damaged.

Author contributions

Conceptualization, J.C. and A.N.; methodology, J.C. and A.N.; formal analysis, J.C., A.N. and L.K; investigation, L.K.; writing – original draft preparation, J.C., A.N. and L.K.; writing – review and editing, J.C. and A.N. All authors have read and agreed to the published version of the manuscript.

References

[1] Drozd K., Walczak M., Szala M., Gancarczyk K. Tribological behavior of AlCrSiN-coated tool steel K340 versus popular tool steel grades. Materials, 2020, 13(21), 4895.
[2] Panchenko S., Gerlici J., Vatulia G., Lovska A., Rybin A., Kravchenko O. Strength assessment of an improved design of a tank container under operating conditions. Communications - Scientific Letters of the University of Žilina, 2023, 25, 3, B186-B193.
[3] Szala M., Szafran M., Matijošius J., Drozd K. Abrasive Wear Mechanisms of S235JR, S355J2, C45, AISI 304, and Hardox 500 Steels Tested Using Garnet, Corundum and Carborundum Abrasives. Advances in Science and Technology Research Journal, 2023, 17(2), 147-160.
[4] Čėsna J., Golub G., Kukharets S., Hutsol T., Medvedskyi O., Slobodian S., Vadym H., Malaga-Tobola U., Stroianovska L. Substantiation of the radius of curvature of the chisel plow point of the working bodies of tillage implements. Agricultural Engineering, 2022, 26(1), 231-241.

[5] Lonkwic P., Usydus I., Tofil A., Krakowski T., Ruta H., Pieniak D. Case study on numerical optimization of a disc bush in the disc harrow and welding processes. Mechanika, 2021, 27(6), 513-520.
[6] Meneghetti G., Campagnolo A. State-of-the-art review of peak stress method for fatigue strength assessment of welded joints. International Journal of Fatigue, 2020, 139, 105705.
[7] Nadykto V., Kiurchev S., Chorna T., Hutsol T., Mudryk K., Głowacki S., Rud A., Shevtsova A., Ryabov I., Szwedziak K. Experimental studies on the operation of agricultural crops mowing unit with simultaneous chopping and incorporation of stubble into the soil. Agricultural Engineering, 2023, 27 (1), 301-313.
[8] Sejkorova M., Hurtova I. Engine oil analysis - Effective instrument to evaluate reliability of tractor engines. Engineering for Rural Development, 2019, 18, 971-976.
[9] Shahgholi G., Moinfar A., Khoramifar A., Sprawka M., Szymanek M. Investigating the effect of tractor's tire parameters on soil compaction using statistical and Adaptive Neuro-Fuzzy Inference System (ANFIS) methods. Agriculture, 2023, 13, 259.
[10] Kopčanová S., Sejkorová M., Kučera M., Hnilicová M. Wear of hydraulic system components assessment based on the analysis of hydraulic oil degradation degree. Przemysl Chemiczny, 2020, 99(9), 1399-1403.
[11] Przystupa K., Ambrożkiewicz B., Litak G. Diagnostics of transient states in hydraulic pump system with Short Time Fourier Transform. Advances in Science and Technology Research Journal, 2020, 14(1), 178-183.
[12] Faraj R., Graczykowski C., Hinc K., Holnicki-Szulc J., Knap L., Senko J. Adaptable pneumatic shock-absorber. 8th Conference on Smart Structures and Materials, SMART 2017 and 6th International Conference on Smart Materials and Nanotechnology in Engineering, SMN 2017, 2017, 2017-January, 86-93.
[13] Jilek P., Berg J., Tchuigwa B.S.S. Influence of the Weld Joint Position on the Mechanical Stress Concentration in the Construction of the Alternative Skid Car System's Skid Chassis. Applied Sciences, 2022, 12(1), 397.
[14] Panchenko S., Gerlici J., Vatulia G., Lovska A., Ravlyuk V., Harusinec J. Studying the load of composite brake pads under high-temperature impact from the rolling surface of wheels. EUREKA, Physics and Engineering, 2023, 4, 155-167.
[15] Ulbrich D., Selech J., Kowalczyk J., Jóźwiak J., Durczak K., Gil L., Pieniak D., Paczkowska M. Reliability analysis for unrepairable automotive components. Materials, 2021, 14(22), 7014.
[16] Pieniak D., Jedut R., Gil L., Kupicz W., Borucka A., Selech J., Bartnik G., Przystupa K., Krzysiak Z. Comparative evaluation of the tribological properties of polymer materials with similar shore hardness working in metal–polymer friction systems. Materials, 2023, 16, 573.
[17] Bujna M., Prístavka M., Lee C.K., Borusiewicz A., Samociuk W., Beloev I., Malaga-Tobola U. Reducing the probability of failure in manufacturing equipment by quantitative FTA analysis. Agricultural Engineering, 2023, 27(1), 255-272.
[18] Blatnický M., Dižo J., Molnár D., Droździel P. Design of a manipulator of a conveyor for bulk materials - calculation of the center of gravity of the conveyor. Scientific Journal of Silesian University of Technology. Series Transport, 2022, 117, 43-56.
[19] Dąbrowska K., Nowak R., Rumianek P., Seńko J. Construction and validation of simulation models of samples made from 316L steel by applying additive technique. Materials, 2022, 15(18), 6244.
[20] Lonkwic P., Różyło P., Usydus I. Numerical analysis and experimental investigation of disk spring configurations with regard to load capacity of safety progressive gears. Applied Computer Science, 2016, 12(3), 5-16.
[21] Gerlici J., Sakhno V., Yefymenko A., Verbitskii V., Kravchenko A., Kravchenko K. The stability analysis of two-wheeled vehicle model. MATEC Web of Conferences, 2018, 157, 01007.
[22] Jilek P., Cerman J. Design of sliding frame system for two-wheeled vehicle. Transport Means - Proceedings of the International Conference, 2020, 136-141.
[23] Podkowski K., Barszcz Z., Seńko J. FEM (Finite element method) numeric analyses of the syrenka S201 car model. Lecture Notes in Mechanical Engineering, 2017, 415-421.
[24] Decker Ž., Tretjakovas J., Drozd K., Rudzinskas V., Walczak M., Kilikevičius A., Matijosius J., Boretska I. Material's strength analysis of the coupling node of axle of the truck trailer. Materials, 2023, 16, 3399.

[25] Lovska A., Stanovska I., Nerubatskyi V., Hordiienko D., Zinchenko O., Karpenko N., Semenenko Y. Determining features of the stressed state of a passenger car frame with an energy-absorbing material in the girder beam. Eastern-European Journal of Enterprise Technologies, 2022, 5(7-119), 44-53.
[26] Dižo J., Blatnický M., Sága M., Harušinec J., Gerlici J., Legutko S. Development of a new system for attaching the wheels of the front axle in the cross-country vehicle. Symmetry, 2020, 12, 1156.
[27] Godwin R.J., O'Dogherty M.J. Integrated soil tillage force prediction models. Journal of Terramechanics, 2007, 44(1), 3-14.
[28] Krzysiak Z., Samociuk W., Zarajczyk J., Kaliniewicz Z., Pieniak D., Bogucki M. Analysis of the sieve unit inclination angle in the cleaning process of oat grain in a rotary cleaning device. Processes, 2020, 8, 346.
[29] Mouazen A.M., Nemenyi M. Finite element analysis of subsoiler cutting in non-homogeneous sandy loam soil. Soil & Tillage Research, 1999, 51(1-2), 1-15.
[30] Bulzak T., Winiarski G., Wójcik Ł., Szala M. Application of numerical simulation and physical modeling for verifying a cold forging process for rotary sleeves. Journal of Materials Engineering and Performance, 2022, 31(3), 2267-2280.
[31] Cepova L., Cep R., Chalko L., Dvorackova S., Trochta M., Rucki M., Beranek L., Mizera O., Chyshkala V. The Effect of Cutting Tool Geometry on Surface Integrity: A Case Study of CBN Tools and the Inner Surface of Bearing Rings. Applied Sciences, 2023, 13(6), 3543.
[32] Winiarski G. Theoretical and experimental study on the effect of selected parameters in a new method of extrusion with a movable sleeve. Materials, 2022, 15(13), 4585.
[33] Arvidsson J., Hillerstrom O. Specific draught, soil fragmentation and straw incorporation for different tine and share types. Soil and Tillage Research, 2010, 110(1), 154-160.
[34] Talarczyk W., Łowiński Ł. Konstrukcja i zastosowanie głęboszy. Technika rolnicza ogrodnicza i leśna, 2018, 5, 19-23.
[35] Mouazen A.M., Ramon H. Development of on-line measurement system of bulk density based on on-line measured draught, depth and soil moisture content. Soil &Tillage Research, 2006, 86(2), 218-229.
[36] Hamza M.A., Anderson W.K. Combinations of ripping depth and tine spacing for compacted sandy and clayey soils. Soil & Tillage Research, 2008, 9(2), 213-220.
[37] Wang X., Zhang S., Pan H., Zheng Z., Huang Y., Zhu R. Effect of soil particle size on soil subsoiler interactions using the discrete element method simulations. Biosystems Engineering, 2019, 182, 138-150.
[38] Sadek M.A., Chen Y., Liu J. Simulating shear behavior of a sandy soil under different soil conditions. Journal of Terramechanics, 2011, 48(6), 451-458.
[39] Wang X., Li P., He1 J., Wei W., Huang Y. Discrete element simulations and experiments of soil-winged subsoiler interaction. International Journal of Agricultural and Biological Engineering, 2021, 14(1), 50-62.
[40] Badegaonkar U., Dixit G., Pathak K.K. An experimental investigation of cultivator shank shape on draft requirement. Archives of Applied Science Research, 2010, 2(6), 146-255.
[41] Celik A., Raper R.L. Design and evaluation of ground-driven rotary subsoilers. Soil & Tillage Research, 2012, 124, 203-210.
[42] Tamas K., Jori I.J., Mouazen A.M. Modelling soil-sweep interaction with discrete element method. Soil & Tillage Research, 2013, 134, 223-231.
[43] Jiang X., Tong J., Ma Y., Sun J. Development and verification of a mathematical model for the specific resistance of a curved subsoiler. Biosystems Engineering, 2020, 190, 107-119.
[44] Bandalana E.P., Salokhe V.M., Guptaa C.P., Niyamapa T. Performance of an oscillating subsoiler in breaking a hardpan. Journal of Terramechanics, 1999, 36, 117-125.
[45] Topakci M., Celik H.K., Canakci M., Rennie A.E.W., Akinci I., Karayel D. Deep tillage tool optimization by means of finite element method: Case study for a subsoiler tine. Journal of Food, Agriculture & Environment, 2010, 8(2), 531-536.
[46] Kadam A., Chhapkhane N. Design and analysis of subsoiler. International Journal of Modern Trends in Engineering and Science, 2017, 4(1), 11-14.
[47] Hang C., Gao X., Yuan M., Huang Y., Zhu R. Discrete element simulations and experiments of soil disturbance as affected by the tine spacing of subsoiler. Biosystems Engineering, 2018, 168, 73-82.